International Science and Technology Journal
المجلة الدولية للعلوم والتقنية
Volume 38 العدد
Part 2 المجلد
ISTJ

Material Demand and Sustainability Risks in Scaling Emerging Perovskite Photovoltaics for Global Energy Deployment

http://www.doi.org/10.62341/istj-vol38-2-irego74

Received	**2026/06/01**	**تم استلام الورقة العلمية في**
Accepted	**2026/06/19**	**تم قبول الورقة العلمية في**
Published	**2026/06/20**	**تم نشر الورقة العلمية في**

Material Demand and Sustainability Risks in Scaling Emerging Perovskite Photovoltaics for Global Energy Deployment

Abrar Arafa
Chemical Engineering Department, University of Tripoli, Libya
ab.arafa@uot.edu.ly

Abstract

Photovoltaics (PVs) deployment offers a viable pathway to fulfilling a substantial amount of the global energy demand. Perovskites are expected to reach commercial stage manufacture soon. Driven by lead-based perovskites, lab-scale power conversion efficiencies (PCEs) have reached 27%, surpassing the PCEs of conventional silicon-based PVs (20 – 24%). Yet, the total PVs material demands required to fulfil projected energy deployment remain unquantified. Herein, data from 5 perovskite PVs were collected, each of a unique architecture, and material demands were estimated based on PCEs and market share predictions, assuming a commercial module lifespan of 25 years. Perovskite PVs' Market share was varied as a portion of a famous scenario that projects PVs deployment throughout the upcoming 25 years, namely the Teske 1.5ºC scenario. Material demands differ depending on the architecture of each device. Results suggest that supply risks associated with tin, iodine, indium, and silver may delay commercial deployment of perovskite PVs. Iodine exhibits a higher supply risk than has been acknowledged in literature. Sensitivity analyses underscore that entering the commercial market at elevated PCEs can significantly maximise material savings. These insights can be used as a bassline for life cycle assessments, guiding the selection of optimal module architecture from both economic and environmental perspectives.
This scientific manuscript was presented at the sessions of the

International Science and Technology Journal
المجلة الدولية للعلوم والتقنية
Volume 38 العدد
Part 2 المجلد
المجلة الدولية للعلوم والتقنية
ISTJ

Material Demand and Sustainability Risks in Scaling Emerging Perovskite Photovoltaics for Global Energy Deployment

http://www.doi.org/10.62341/istj-vol38-2-irego74

International Renewable Energy, Gas, Oil and Climate Change Conference "iREGO" in the period of April 25-27, 2026. Tripoli - Libya

Keywords: perovskites; power conversion efficiency; material demand sustainability; supply risk.

احتياجات المواد ومخاطر الاستدامة في توسيع نطاق الخلايا الشمسية البيروفسكيتية الناشئة لتلبية احتياجات الطاقة العالمية

أبرار عرفة
قسم الهندسة الكيميائية، جامعة طرابلس، ليبيا
ab.arafa@uot.edu.ly

الملخص:

توفر تقنية الخلايا الكهروضوئية (الشمسية) طريقاً قابلاً للتطبيق لتلبية جزء كبير نسبياً من الاحتياج العاملي للطاقة. قريباً من المتوقع أن تصل تقنية البيروفسكيت إلى مرحلة التصنيع التجاري. بسبب وجود الرصاص في تركيبة الخلايا الضوئية المكونة من مادة البيروفسكيت، وصلت كفاءة تحويل الطاقة في نطاق المعامل إلى 27%، متجاوزة كفاءة تحويل الطاقة للخلايا الشمسية التقليدية المصنعة من مادة السيليكون (20–24%). ومع ذلك، لا يزال احتياج المواد اللازمة من هذه الخلايا لتلبية الاحتياجات المستقبلية للطاقة حول العالم مجهولاً. في هذا العمل، تم جمع بيانات من 5 خلايا شمسية (وحدات) مكونة من مادة البيروفسكيت، كل منها بتصميم مختلف، وتم تقدير احتياجات المواد المستخدمة في كل وحدة بناء على كفاءة تحويل طاقة محددة، مع عمر افتراضي يبلغ 25 عاما لكل وحدة. تفاوتت الحصة السوقية المتوقعة للبيروفسكيت في سيناريو شهير بتوقعاته للحصص السوقية لبعض الطاقات المتجددة، واختلفت احتياجات المواد حسب تصميم الوحدة. أشارت النتائج المستندة على السناريو المستخدم إلى أن مخاطر الإمداد المتعلقة بالقصدير واليود

Material Demand and Sustainability Risks in Scaling Emerging Perovskite Photovoltaics for Global Energy Deployment

http://www.doi.org/10.62341/istj-vol38-2-irego74

والإنديوم والفضة كانت أعلى من المتوقع وقد تكون سبب في تأخر الاستخدام التجاري لهذه التقنية. أوضحت التحليلات أن الدخول إلى السوق التجارية بمعدلات كفاءة تحويل طاقة عالية يمكن أن يقلل استهلاك المواد في الوحدة الواحدة بشكل ملحوظ. يمكن استخدام نتائج هذا العمل لدراسة دورة الحياة، مما يساهم في اختيار التصميم الأمثل للوحدات من كلا الجانبين الاقتصادي والبيئي.

وقد تم عرض هذه الورقة العلمية في جلسات المؤتمر الدولي للطاقة المتجددة والنفط والغاز وتغير المناخ "أيريقو" في الفترة 25–27 ابريل 2026م. طرابلس – ليبيا

الكلمات المفتاحية: البيروفسكايت؛ كفاءة تحويل الطاقة؛ استدامة الطلب على المواد؛ مخاطر الإمداد

1. Introduction

Global primary energy consumption continues to rise, surpassing 600 EJ in 2024 [1], driven by population growth and rapid industrial expansion. Despite progress in renewable deployment, energy production remains dominated by carbon-based fuels, sustaining high levels of anthropogenic carbon dioxide (CO_2) emissions. Atmospheric CO_2 concentrations have now exceeded 420 ppm, well beyond the planetary boundary threshold [2], and global surface temperatures are consistently more than 1.1°C above the 20th-century baseline [3]. These trends have intensified climate-related disasters, underscoring the urgency of achieving the Paris Agreement's target of limiting warming to 1.5 °C by mid-century [4]. The challenge of achieving net-zero by 2050, while satisfying global energy demand, cannot be achieved without sustainable renewable technologies and decarbonization strategies.

Among renewable technologies, solar photovoltaics (PVs) have emerged as a foundation of climate mitigation scenarios. Their rapid cost reductions and scalability have enabled deployment at rates surpassing earlier projections [5], [6], making PVs cheaper than fossil fuel alternatives in most regions [7]. Crystalline silicon (c-Si) devices remain the dominant commercial technology, with record

http://www.doi.org/10.62341/istj-vol38-2-irego74

efficiencies above 27% [8]. Thin-film alternatives such as copper indium gallium selenide and cadmium telluride have also matured, achieving efficiencies over 22% [9]. More recently, perovskite PVs have revolutionized the field, offering high power conversion efficiencies (PCE) through low-cost, solution-based manufacturing methods. Certified perovskite solar cells (PSCs) have reached efficiencies of 27% [10], with modules exceeding 21% [11], highlighting their potential to complement established PV technologies in the global energy mix. Compared with Si-based PVs, perovskites can achieve higher PCEs with lower energy consumption and reduced environmental footprint [12]. Despite these advances, perovskite PVs face critical sustainability challenges. Their instability under heat, oxygen, and moisture, as well as reliance on toxic materials such as lead (Pb) and hazardous solvents, raise concerns for large-scale deployment [13]. Addressing these issues is essential for enabling perovskite solar modules (PSMs) to contribute meaningfully to decarbonization goals.

This work evaluates the sustainable potential of perovskite PVs for large-scale market integration by analysing whether future deployment may be constrained by materials availability. Using data from 5 promising perovskite architectures, the material requirements per square meter to meet projected energy demand between 2025 and 2050 under the Teske 1.5 °C climate mitigation scenario [4] was estimated. Sensitivity analyses were conducted to quantify how variations in solar PV market share and PCEs of PSMs affect overall materials demand and sustainability.

2. Materials and Methods

2.1. Selection of Climate Change Scenario

Fig.1 shows the predictions of global cumulative installed PV capacity (in GW) from various reports and potential scenarios.

Material Demand and Sustainability Risks in Scaling Emerging Perovskite Photovoltaics for Global Energy Deployment

http://www.doi.org/10.62341/istj-vol38-2-irego74

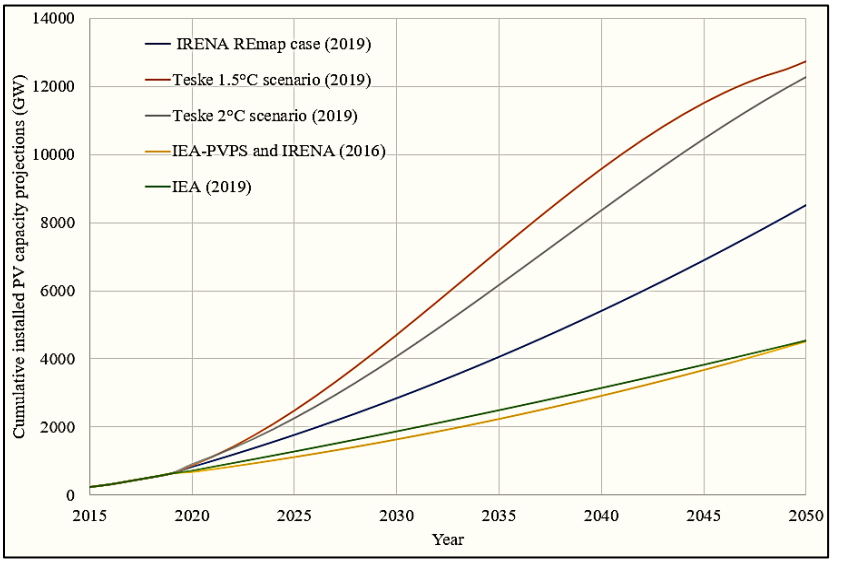

Figure (1): Predicted global cumulative installed PV capacity (GW) during 2015 – 2050 across various climate change mitigation scenarios. Data adapted from the Teske et al. scenarios [4], IRENA REmap case [6], IEA-RVPS and IRENA [5], and IEA new policies [14].

Global installed PV capacity reached 760 GW in 2020, surpassing IEA-PVPS, IRENA [5], and IEA policies [14] projections of 670–710 GW, which indicates underestimation of future installations. IRENA's REmap scenario [6] overpassed by 58 GW, making its early estimates steeper than the actual case. Teske et al. [4] projected about 250 GW above actual and 3 times higher than IEA/IRENA estimates. Teske's scenarios, targeting 1.5°C and 2°C by 2050, depend on 100% renewables with PV contribution of 48–49%. Despite their ambition, only wind and PV are currently on track [15]. PV's LCOE ($0.057/kWh avg.) dropped below carbon-based fuels ($0.055–0.148/kWh avg.) [16], supporting further deployment. PV's share among renewables rose from 9.6% (175 GW) in 2014 to >27% in 2020, with this 585 GW increase, PV deployment capacity may meet future energy targets. Teske's 1.5°C scenario offers stronger climate mitigation and informs peak material demand between 2025–2050. It was selected to model PV deployment and perovskite PV demand, assuming 0–15% linear

http://www.doi.org/10.62341/istj-vol38-2-irego74

market growth from 2025 to 2050, with no module replacement needed, provided a commercially viable lifespan of 25 years is attained.

2.2. Projections for Global PV Deployment Capacity

A 3rd degree polynomial equation was fit to the Teske 1.5ºC scenario using the data in Table 1.

Table (1): Worldwide projections of PV capacity under Teske 1.5 ºC scenario, reproduced from Teske et al [4].

Year	2015	2025	2030	2040	2050
PV Capacity (GW)	225	2829	5133	10,017	12,684

Annual PV installations from 2025 to 2050 were estimated using (1) where y_n and y_{n-1} represent the cumulative installed PV capacities for a given (current) and preceding years, respectively.

$$\text{Annual PV installation } (y'_n) = y_n - y_{n-1} \quad (1)$$

Assuming a linear growth of perovskite market share from 0 to 15% between 2025 and 2050, the percentage growth in market share for any given year ($MS._n$), was calculated using (2) where x_i and x_f denote the initial (0.0) and final (0.15) market shares. While t_i: initial year (2025), t_n: targeted year, and t_f: final year (2050).

$$MS._n = \left(\left(\frac{x_f - x_i}{t_f - t_i}\right) * (t_n - t_i) + x_i\right) * 100\ \% \quad (2)$$

Annual deployment metric for perovskite-based PVs (Y'_p) across the 2025-2050 span were computed using (3):

$$Y'_{P(n)} = MS._n * y'_n \quad (3)$$

To determine the cumulative perovskite PV deployment ($Y_{P(n)}$) for any year between 2025 and 2050, the annual installations were summated sequentially using (4).

$$Y_{P(n)} = \sum_i^n Y'_{P(n)} \quad (4)$$

The required unit area (m^2) per GW capacity generated by PSMs was estimated using (5). Which incorporated E_S, the Earth's surface

http://www.doi.org/10.62341/istj-vol38-2-irego74

area 510.1 trillion m^2, *I* the global incident solar energy of 120 million GW, and Ƞ which is the PV module efficiency taken as 0.2.

$$\text{Specific perovskite module area } (A_{SPM}) = \frac{E_S}{I * \eta} \quad (5)$$

Afterwards, the PSM total surface area needed annually to meet projected energy demand was computed using (6).

$$\text{Perovskite module area } (A'_{PM}) = A_{SPM} * Y'_{P(n)} \quad (6)$$

Consequently, the cumulative land area dedicated to perovskites PVs in any target year represents the running total of such yearly installations.

For clarity across subsequent sections, references to a "15% market share" denote a deployment trajectory that scales linearly from 0 % at 2025 to 15 % market share in 2050.

2.3. Selection of PSM Devices' Materials and Architectures

Data regarding the manufacturing steps and deposited materials per unit area were sourced from literature focused on scalable PSM fabrication. The 5 representative devices selected (Fig. 2) were selected based on availability of data sufficient for calculating material requirements and established module-scale fabrication method. Reported PCEs were also considered to assess the feasibility of achieving the assumed 20% efficiency threshold for competitive commercialisation. Slot-die coating method was used for all devices. Device descriptions, active areas, efficiencies, and stability data are summarized in Table 2.

Table (2): Description of coating method, PCE, stability, and active area (A_c) of the 5 identified devices.

Device	Description	PCE %	Stability	A_c (cm^2)
1 [17]	Flexible R2R	12.2	120 min.	0.09
2 [18]	Rigid	12.2	> 1 year.	1.5
3 [20]	Rigid	14.6	-	100
4 [21]	Flexible R2R	11.7	-	0.1
5 [22]	Rigid S2S	23.8	100 hours	1

Material Demand and Sustainability Risks in Scaling Emerging Perovskite Photovoltaics for Global Energy Deployment

http://www.doi.org/10.62341/istj-vol38-2-irego74

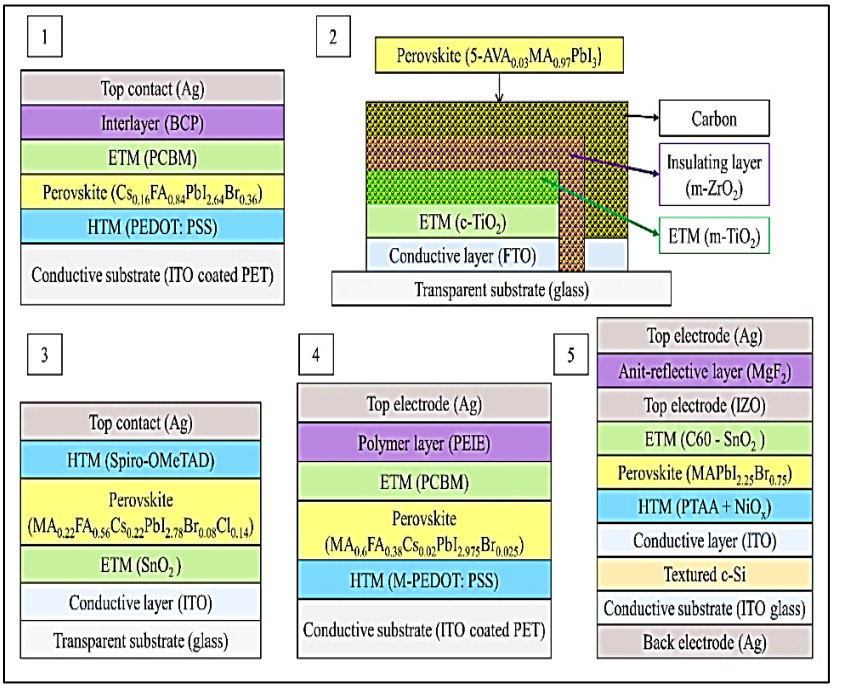

Figure (2): Structural schematics of the 5 PSM device architectures evaluated in this work (indexed 1-5 in the upper left corners). (1): planar (P-I-N) configuration adapted from D. Burkitt et al.[17]. (2): mesoscopic carbon stack adapted from A. Verma et al. [18] and F. De Rossi et al. [19]. (3): planar (N-I-P) configuration adapted from L. Gao et al. [20]. (4): a planar (P-I-N) configuration adapted from J. Kim et al. [21]. (5): tandem (c-Si/ perovskite) adapted from A. Subbiah et al. [22]. Abbreviations: c-/ m-TiO_2: compact/ mesoporous TiO_2, BCP: bathocuproine, MgF_2: magnesium fluoride, PCBM: PCBM60, 5-AVA: 5-aminovaleric acid iodide, , M-PEDOT: PSS: modified PEDOT: PSS, PEIE: polyethyleneimine ethoxylate.

2.4. Perovskite Solar Modules Manufacturing Data and Materials Quantification

Fabrication data for perovskite solar modules were compiled from slot-die coating parameters and used to calculate material requirements through a developed nine-step analytical framework. Important parameters affecting the manufacturing process and the

http://www.doi.org/10.62341/istj-vol38-2-irego74

purpose of collection of each is listed in Table 3. Notably, this assessment excludes the material demands from secondary components of the PSM such as module wiring, encapsulation materials, and junction-boxes.

Table (3): Essential parameters of PSMs fabricated via slot-die coating method alongside the purpose of collection.

Parameter	Purpose (analytical role)
Coating width (m)	Determines the total surface area printed per unit time.
Pump rate (ml min^{-1})	Sets the ink flow rate to estimate mass deposition density.
Coating rate (m min^{-1})	Quantifies the area printed over time.
Wet film thickness (m)	Quantifies the initial fluid volume deposited per m^2.
Dry film thickness (m)	A measure to the final active area thickness after evaporation and annealing.
Substrate material	Specifies the base layer.
Substrate resistivity	Identifies the relative thickness of the substrate material.
Electron transport material	Identifies the chemical composition of the ETL.
Hole transport material	Identifies the chemical composition of the HTL.
Perovskite (absorber) material	Identifies the specific stoichiometry of the active layer.
Precursor Solution Concentration	Details the molar ratios and solute-to-solvent formula.
Material Supplier	Provides commercial traceability for physical and/or chemical properties.
Contact material	Identifies the material used as a back electrode.
Electrode thickness (µm)	Indicates the amount of contact layer deposited.

http://www.doi.org/10.62341/istj-vol38-2-irego74

2.5. Projecting Future Material Demands

Future material consumption, in kg, from 2025 to 2050 is modelled by applying the estimated deposited material per unit area (M_D) of each architecture to (7).

$$Material\ demand = A'_{PM} * \frac{M_D}{1000} \quad (7)$$

The total projected solvent requirements, in litres, are calculated by the same approach V_D (volumetric deposition density) instead of M_D in (7). To compute the cumulative material demand across the entire forecast period, these annual metrics are integrated into (4).

2.6. Market Share and Efficiency Sensitivity Analyses

To isolate the impact of static baselines for both PCEs and market share, sensitivity analyses were performed. First, market share value was held constant while the module PCE is stepped though various benchmarks of 17 %, 23 % and 26 %. Then, the core PCE is fixed at 20 % while market share targets are adjusted from 0 % at 2025 to 10 % and 20 % by 2050.

3. Results and Discussion

3.1. Photovoltaic Installation Under Teske 1.5oC Scenario

Perovskite PVs offer relatively high PCEs but remain challenged by long-term stability. Recent advances demonstrate promising stabilised performance, with several pilot scale deployments, reported in 2022 – 2025. Kadro et al. [26] projected thin-film PVs to rise from 0.6% in 2020 to 9.3% by 2030, equivalent to 2.7 GW if perovskites were to capture the entire thin-film share. The 15% market share projection by 2050 remains conservative compared to the rapid advances in efficiency and stability, but also ambitious due to current limited deployment. Fig. 3 shows annual PV installations under the Teske 1.5°C pathway. Deployment peaks in 2042, with steady growth from 2025–2037 followed by slower expansion in the 5 terminal years.

Material Demand and Sustainability Risks in Scaling Emerging Perovskite Photovoltaics for Global Energy Deployment

http://www.doi.org/10.62341/istj-vol38-2-irego74

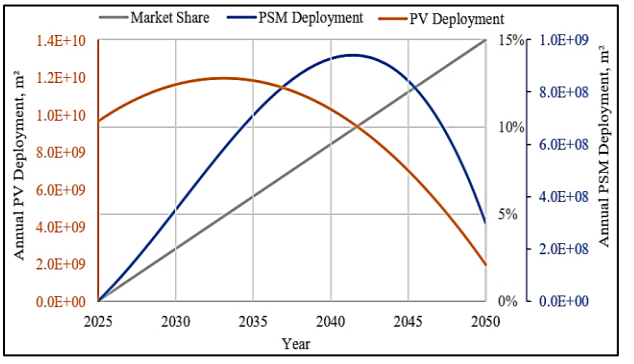

Figure (3): Predicted annual global PV deployment under Teske 1.5ºC scenario and corresponding 15% PSM market share trajectory by 2025.

Meeting this scenario requires 1.56×10^{10} m² of PSMs to deliver 661 GW by 2050, representing a fraction of the 3×10^{11} m² needed for all PV technologies combined. Peak annual PSM deployment alone would cover 9.4×10^{8} m². This scale highlights the substantial material demands associated with meeting the projected energy capacity from perovskites.

3.2. Materials Demand for PSMs Deployment

Fig. 4 shows that, for all 5 devices, substrate mass dominates overall weight, with glass-based modules imposing significant emissions burdens compared to lighter polyethylene terephthalate (PET) substrates. At equal substitution, 1 m² of glass modules can occupy the space of 7–16 PET modules, underscoring the transport and reverse-logistics advantage of flexible devices. Device 2 (hole transport layer (HTL)-free carbon stack) exhibited the highest deposited material intake (93 g m^{-2}) among the other devices (1–9 g m^{-2}), due to infiltration requirements of porous electron transport layer (ETM) and carbon layers. Device 3 consumed the least materials, with 99.9% of its mass in the indium tin oxide (ITO)-coated glass substrate. The tandem device (5) weight was governed by the ITO substrate and the c-Si bottom cell, while flexible roll-to-roll (R2R) devices (1 and 4) were thinner owing to deposition on 175 µm PET substrates.

http://www.doi.org/10.62341/istj-vol38-2-irego74

Solvent consumption correlates with materials consumption. Device 2 required 85 ml m^{-2}, primarily toxic GBL (γ-butyrolactone), while Device 3 consumed only 5 ml m^{-2}. Devices 1 and 3 incorporated safer DMSO (dimethyl sulfoxide)/IPA (isopropanol) but still relied on problematic solvents (toluene, chlorobenzene). Device 4 used hazardous DMF (n-dimethylformamide) and chlorobenzene. Overall, device 5 employed fewer toxic systems but significant volumes of toxic and volatile ACN (acetonitrile). Substitution of these solvents with sustainable alternatives remains critical for industrial scalability.

Pb content varied substantially. Device 2 contained the highest Pb loading (7.25 g m^{-2} as PbI_2), consistent with its thicker absorber, while Device 5 followed with 1.11 g m^{-2}. Devices 1 and 4 used intermediate amounts, 0.50–0.76 g m^{-2}, and Device 3 the used least, 0.05 g m^{-2}. Pb incorporation strongly influenced PCE: Device 2 achieved 12.2% at 1.5 cm^2, while Device 5 reached 23.8% at 1 cm^2. Notably, Device 2 demonstrated stability over a year without encapsulation, contrasting with the shorter lifetimes of other architectures. Full recoverability of the perovskite layer would simplify Pb management compared to sensitive architectures like R2R. Ultimately, Pb toxicity must be controlled through strict workplace exposure limits, robust encapsulation or absorbing materials for end users, and complete Pb recovery at the module's end-of-life.

Mass fraction analysis (Fig. 5) confirmed that conductive substrates account for 97–99.9% of device weight, with active layers contributing to less than 3%. These differences highlight the disproportionate role of substrates and solvents in environmental impact. While Device 2 benefits from low-cost carbon electrodes and extended stability, Device 5's tandem design relies on expensive and less sustainable components.

Material Demand and Sustainability Risks in Scaling Emerging Perovskite Photovoltaics for Global Energy Deployment

http://www.doi.org/10.62341/istj-vol38-2-irego74

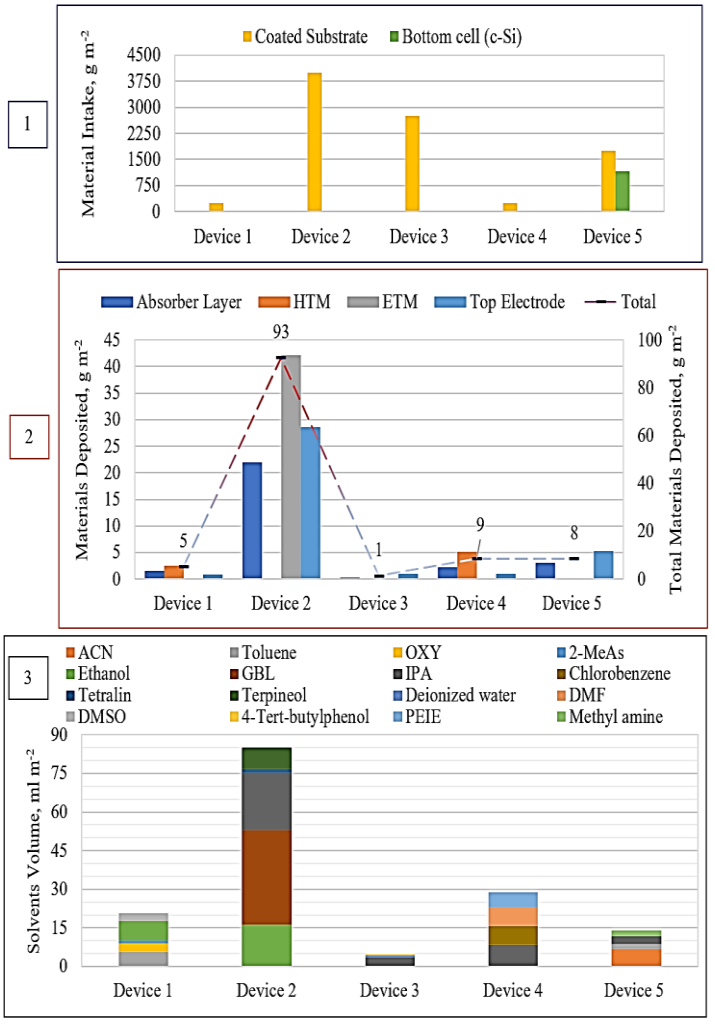

Figure (4): Comparartive breakdown of area-normalised material requiremenets for the 5 anlaysed devices: (1) Substrate mass profiles for all architecutures alonside the silicicon requirement from device 5; (2) specific layer-by-layer depostion metrics and cumulative mass requirements per device; and (3) total solvent consumption across all 5 fabricated deviced.

Material Demand and Sustainability Risks in Scaling Emerging Perovskite Photovoltaics for Global Energy Deployment

http://www.doi.org/10.62341/istj-vol38-2-irego74

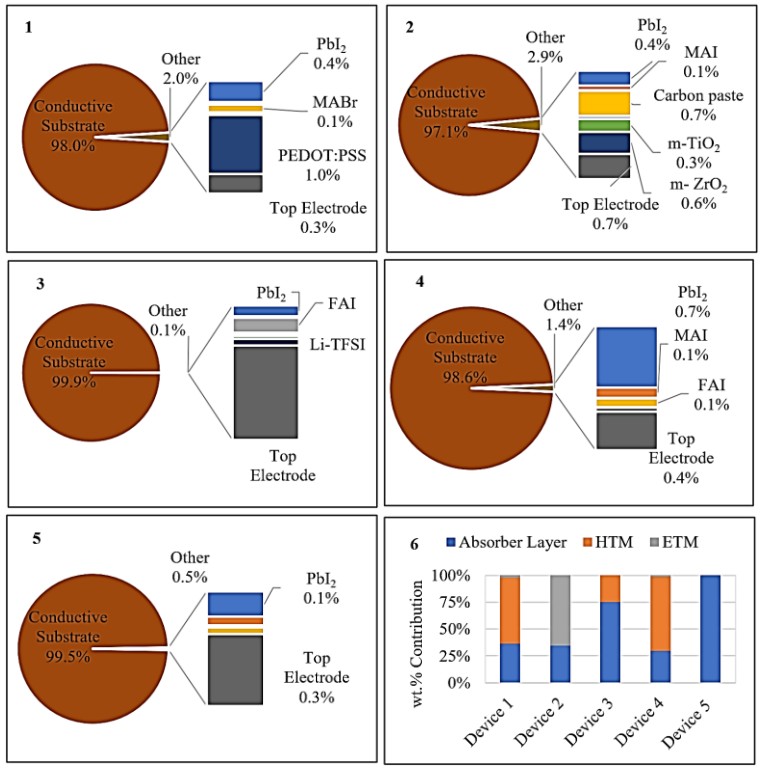

Figure (5): (1-5) Mass fraction (wt.%) distributions of substrate, top electrode, and active layers for devices 1-5 (indexed 1 to 5 in the upper-left corners),with contributions under 0.1 wt.% emitted, (6) isolated mass fractions of individual active layers across all 5 architectures.

Eventually, architecture choice must balance efficiency, stability, and sustainability metrics, as materials demand alone cannot determine commercial viability.

3.3. Material Demands for Projected PSM Deployment

The annual and cumulative material demand projections for device 1 are shown in Fig. 6 and 7, respectively. The same trend was found for devices 2 – 5. The profiles of deposited materials demand largely mirror PV deployment trends, with substrates dominating requirements due to their mass. Even lighter PET substrates in R2R devices remain about 2 orders of magnitude heavier than the active

Material Demand and Sustainability Risks in Scaling Emerging Perovskite Photovoltaics for Global Energy Deployment

http://www.doi.org/10.62341/istj-vol38-2-irego74

layers, emphasizing the thin-film nature of perovskites. Device 2 stands out for its simplified composition—using only MA (methyl ammonium), 5-AVA, I (iodine), and Pb—while avoiding HTMs and metal electrodes, relying instead on carbon paste with carbon contributing to long-term stability.

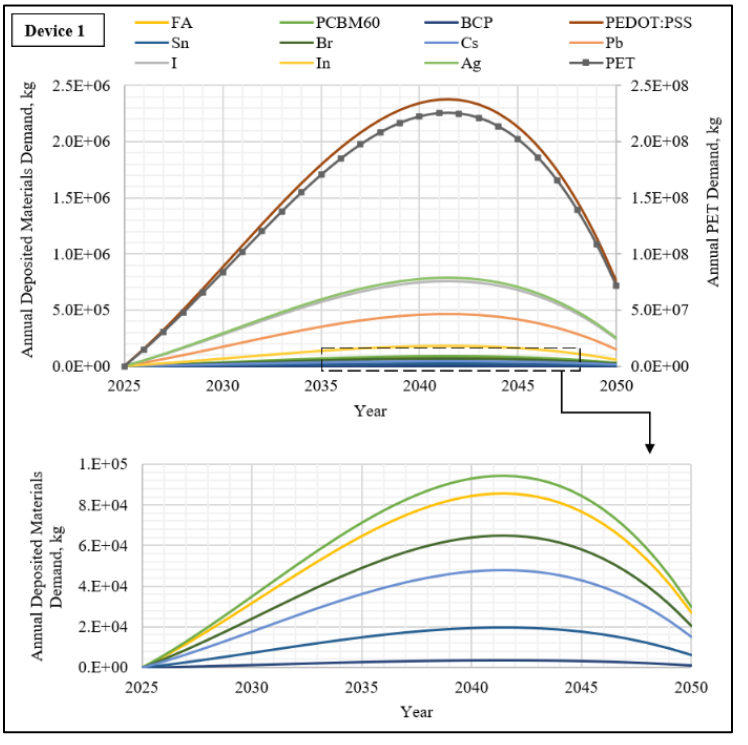

Figure (6): Annual material requirements to sustain perovskite PV deployment projections under the Teske 1.5ºC scenario for device 1 with 20% PCE.

Carbon paste mainly composes of graphite and abundant black carbon. In 2020, the latter production rate reached 1.1 x 10^9 kg, representing a mere 0.34% of known global reserves. Despite its extensive use across various renewable energy sectors, graphite has a 7.4 RSRI (relative supply risk index), current productions capacities remain robust enough to satisfy the overall market demand alongside the projected peak demand of 5x10^6 kg from

Material Demand and Sustainability Risks in Scaling Emerging Perovskite Photovoltaics for Global Energy Deployment

http://www.doi.org/10.62341/istj-vol38-2-irego74

perovskite PVs. Devices 3 and 4 employ more complex multi-cation/anion perovskites. If these specific architectures can attain their superior PCEs paired with extended operational stabilities, then their compositional complexity may be justified due to their raw material availability, price, and life cycle assessment outcomes.

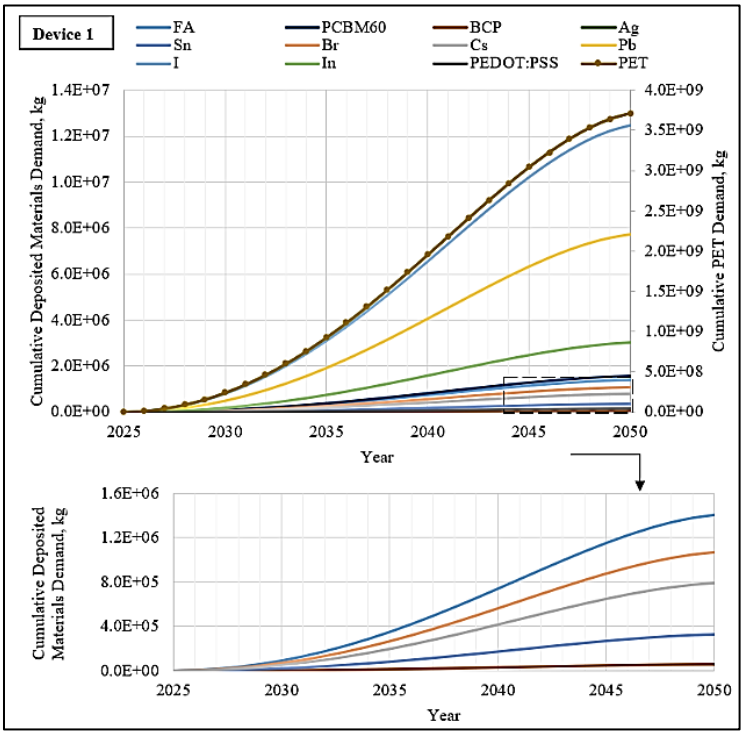

Figure (7): Cumulative material requirements to sustain perovskite PV deployment projections under the Teske 1.5°C scenario for device 1 with 20% PCE.

Associating projected demand with current production rates highlights potential supply risks, requiring mitigation through scaling production, recycling, or substitution. Some materials have undeclared (direct) production data (e.g., BCP, PEIE, PET, etc…), emphasizing the need for careful monitoring of cumulative and peak demands to ensure sustainable deployment. High material usage in HTLs and ETLs can pose cost and environmental challenges, as

Material Demand and Sustainability Risks in Scaling Emerging Perovskite Photovoltaics for Global Energy Deployment

http://www.doi.org/10.62341/istj-vol38-2-irego74

seen with PTAA (poly[bis(4-phenyl)(2,4,6-trimethylphenyl)amine]) in device 5. Architecture 2 avoids most of these issues aside from glass substrate demand, which peaked at about 14% of global flat glass production rate in 2009 and requires progress in recycling to meet future needs. Flexible devices using PET substrates may offer a more viable path if glass supply constraints persist, supported by feasible plastic recycling. Fig. 8 shows the total elements requirements per unit area from each device.

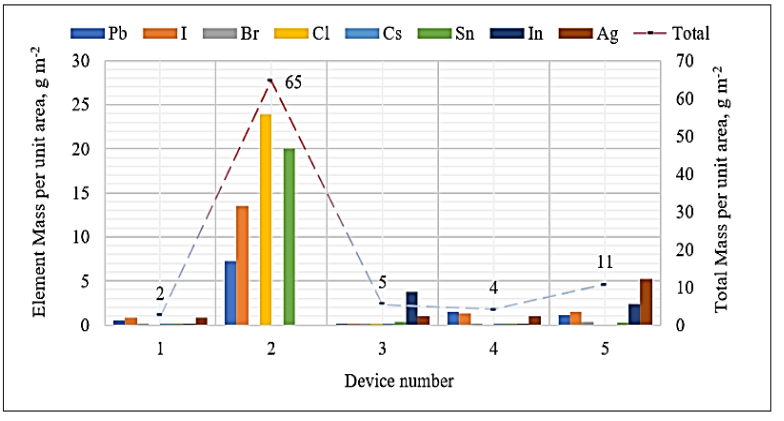

Figure (8): Area-normalised elements demand for each analysed device (1-5).

Overall, projected material demand will pressure raw material production, and reliance on critical or scarce elements could disrupt large-scale perovskite deployment.

Table 4 details the peak annual demand for specific elements alongside their share of 2020 global production rates. Also, it identifies the year at which the cumulative material demand would deplete an equivalent quantity of the 2020 production, assuming PSMs capture 100% the global output, to underscore the resource scarcity and showcase that some critical materials may need substitution sooner than expected.

Material Demand and Sustainability Risks in Scaling Emerging Perovskite Photovoltaics for Global Energy Deployment

http://www.doi.org/10.62341/istj-vol38-2-irego74

Table (4): Projected cumulative elemental demands (kg) for the 5 identified architectures, coupled with their estimated threshold years for intersecting 2020 global production rates. Timelines are categorised by traffic light scores: green represents no intersection or after 2045, amber denotes an intersection period between 2036 and 2045, and red highlights a critical supply intersection between 2025 and 2035.

N	Cumulative Demand (kg)					Intersect Year				
	D 1	D 2	D 3	D 4	D 5	D 1	D 2	D 3	D 4	D 5
Pb	7.7×10^6	1.1×10^8	8.2×10^5	2.3×10^7	1.7×10^7	Never				
I	1.2×10^7	2.1×10^8	3.0×10^6	2.0×10^7	2.3×10^7		2032			
Br	1.1×10^6	0	1.8×10^5	1.1×10^5	4.9×10^6	Never				
Cl	0	3.7×10^8	1.3×10^5	0	0	/				
Cs	7.9×10^5	0	1.2×10^5	1.5×10^5	0	/				
Sn	3.3×10^5	3.1×10^8	5.1×10^6	3.3×10^5	3.3×10^6		2046			
In	3.0×10^6	0	5.9×10^7	3.0×10^6	3.7×10^7	2036	/	2027	2035	2028
Ag	8.1×10^7	1.6×10^7	1.6×10^7	1.3×10^7	8.2×10^7		/			2036

Pb plays a vital role in all device architectures, with a relatively low RSRI (5.5) and strong recycling rates that make its supply secure. About 60% and 80% of Pb production in Europe and the U.S, respectively, come from secondary sources, while China dominates global refined Pb production. Compared with tin (Sn) which has a GWP (global warming potential) of 17.1 kg CO_2-eq/ kg[27], Pb depicts a relatively low GWP (1.3 kg CO_2-eq/ kg). Despite by-products like Zn (zinc) and Ag (silver) affecting market dynamics, projected demand for Pb and Br (barium) from perovskite devices remains negligible compared to current production, posing no risk to global availability. Ag is primarily extracted from copper deposits and argentiferous ores. Driven by expanding industrial applications, global demand for Ag is expected to increase by 37% between 2018 and 2050 [28]. Ag is more critical due to its wide industrial use and limited recycling rates, with c-Si solar panels being major consumers. Recovery at end-of-life or substitution with copper (Cu), nickel (Ni), Zn, or carbon electrodes could ease supply risks [29], though performance trade-offs must be considered. Indium (In) and **I** present greater challenges, with device 2 driving

http://www.doi.org/10.62341/istj-vol38-2-irego74

I demand beyond 2020 production by 2032, and architectures 3 and 5 requiring **In** far above current supply. In's scarcity and reliance on Zn mining make substitution or improved recycling urgent, particularly for flexible substrates where ITO is used. Although **I** is the rarest halogen, it has a moderately low market value, but if device 2 was to be adopted, producers shall prioritise recovering **I** from waste modules.

The primary alternative to Pb, Sn faces escalating global demand; while it remains abundant, it commands a higher cost and carries a medium supply risk. The c-Si PV industry is expected to absorb about 6 x 10^7 kg of Sn by 2025, with an average of 520 kg/MW of Sn is needed [30]. It was found that Sn can be 14 times more expensive than Pb [31]. Moreover, while independent Pb extraction is typically financially viable, standalone Sn mining faces greater commercial burdens. Sn's diverse geographical footprint has preserved it off the critical element lists, though rising industrial demand has recently reported it at high-risk supply [30]. From analysed devices, the highest projected Sn demand resulted in architecture 2 which accounts for 7% of the 2020 production, and the demand will only surpass the 2020 production rate by 2046. Valero et al.[30] showed that Sn demand is expected to surpass its production rate beyond 2042, i.e., the peak demand year in this work. Based on conducted analyses, it can be concluded that projected Sn requirements from the transparent conductive oxide used for perovskite PVs over the next 25 years should not negatively impact its broader global market.

3.4. Sensitivity Analyses: Impact of Market Share and Efficiencies

As shown in Fig. 9, expanding the market share PSMs raises both the annual and cumulative deployment projections, therefore material demands. Conversely, Fig. 10 demonstrates that increasing the PCE of a PSM inherently reduced the projected materials demand, due to the reduction in module area required to generate a specific energy capacity.

Material Demand and Sustainability Risks in Scaling Emerging Perovskite Photovoltaics for Global Energy Deployment

http://www.doi.org/10.62341/istj-vol38-2-irego74

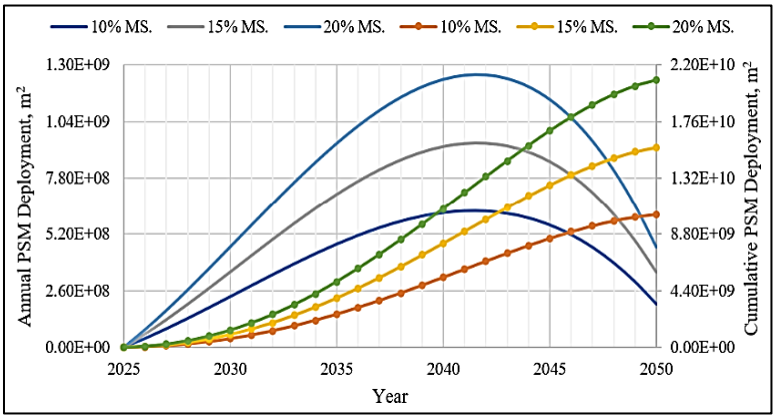

Figure (9): Projected annual (solid lines) and cumulative (scattered lines) PSM deployment trajectories under variable market share (MS.) within the Teske 1.5°C scenario, modelled at a constant 20 % PCE.

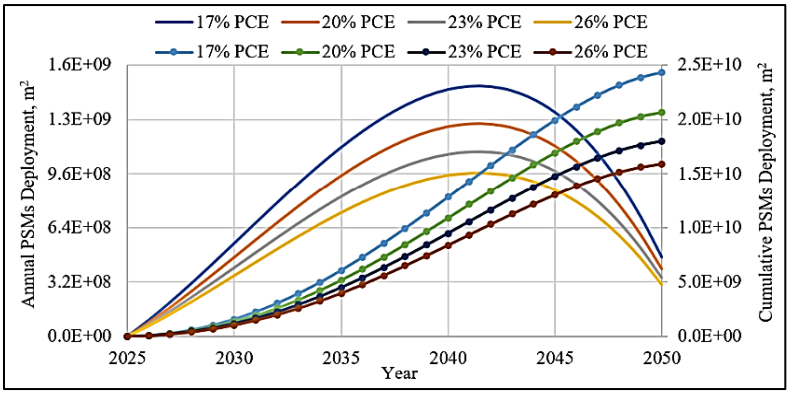

Figure (10): Projected annual (solid lines) and cumulative (scattered lines) PSM deployment trajectories under variable PCEs within the Teske 1.5°C scenario, modelled at a constant 15% MS.

Using 17% PCE as a baseline, raising efficiency to 20% saves 15 wt.% of material use, containing 600 g m^{-2} of glass for architecture 2. Beyond 29% PCE, savings become negligible due to the Shockley–Queisser limit, making 26% an optimal target from both economic and environmental perspectives. At 20% market share by 2050, deploying 17% efficient devices would occupy about 2.4×10^{10} m^2, creating unsustainable pressure on critical materials

http://www.doi.org/10.62341/istj-vol38-2-irego74

like **I**. Results highlight that increasing PCEs significantly reduces substrate and **In** demand, with 26% tandem devices saving 9×10^8 kg of ITO glass and 1.2×10^6 kg of **In**. While **In** use may be limited commercially, these savings underscore the importance of maximising PCEs for sustainable perovskite deployment, alongside broader considerations of cost and environmental impact.

4. Conclusion

To achieve the Paris Agreement 2050 climate goals and meet rising global energy demand, renewable technologies must be deployed at scale and speed. PSMs offer a promising alternative to Si-PVs due to their lower material and manufacturing costs, but their reliance on elements with medium to high supply risk—such as In, I, Ag, and Sn—poses challenges for sustainable deployment. Analysis highlights that device 2, which avoids HTMs and metal contacts, offers strong commercial potential if I use can be mitigated or efficiently recovered. Substitution of Ag with carbon-based electrodes and the adoption of recyclable substrates, whether lightweight plastics or re-manufacturable glass, will be critical to reducing supply risks and enhancing sustainability.

From an environmental perspective, the most pressing concern remains the Pb content of perovskites. While no alternative currently matches Pb in delivering high PCEs, proper encapsulation and recovery strategies are essential to prevent leakage and ensure safe use. Sensitivity analyses confirm that achieving high efficiencies significantly reduces material demand per unit area, easing pressure on critical resources. Although no single architecture can yet be identified as the definitive choice for commercialization, combining low-cost materials, sustainable solvent systems, and long-term stability will accelerate perovskite PV deployment. This study provides a foundation for future life cycle assessments, enabling prioritization of environmental and economic benefits while supporting the development of resilient, low-carbon energy systems.

http://www.doi.org/10.62341/istj-vol38-2-irego74

References

[1] "Global trends – Global Energy Review 2025 – Analysis - IEA." Accessed: Nov. 30, 2025. [Online]. Available: https://www.iea.org/reports/global-energy-review-2025/global-trends

[2] K. Richardson *et al.*, "Earth beyond six of nine planetary boundaries," *Sci Adv*, vol. 9, no. 37, 2023.

[3] K. Calvin *et al.*, "IPCC, 2023: Climate Change 2023: Synthesis Report, Summary for Policymakers. Contribution of Working Groups I, II and III to the Sixth Assessment Report of the Intergovernmental Panel on Climate Change [Core Writing Team, H. Lee and J. Romero (eds.)]. IP…," Jul. 2023, doi: 10.59327/IPCC/AR6-9789291691647.001.

[4] S. Teske, *Achieving the paris climate agreement goals: Global and regional 100% renewable energy scenarios with non-energy GHG pathways for +1.5°C and +2°C*. Springer International Publishing, 2019. doi: 10.1007/978-3-030-05843-2.

[5] IRENA, S. Weckend, IEA-PVPS, A. Wade, and G. Heath, "End-Of-Life Management: Solar Photovoltaic Panels. Photovoltaic Power Systems," p. 100, 2016, Accessed: Nov. 29, 2025. [Online]. Available: https://iea-pvps.org/wp-content/uploads/2020/01/IRENA_IEAPVPS_End-of-Life_Solar_PV_Panels_2016.pdf

[6] IRENA, "Global energy transformation: A roadmap to 2050," *International Renewable Energy Agency*, pp. 1–51, 2019.

[7] "Solar is now 'cheapest electricity in history', confirms IEA." Accessed: Nov. 30, 2025. [Online]. Available: https://www.carbonbrief.org/solar-is-now-cheapest-electricity-in-history-confirms-iea/

[8] H. Tong *et al.*, "Total-area world-record efficiency of 27.03% for 350.0 cm2 commercial-sized single-junction silicon solar cells," *Nature Communications 2025 16:1*, vol.

http://www.doi.org/10.62341/istj-vol38-2-irego74

16, no. 1, pp. 5920-, Jul. 2025, doi: 10.1038/s41467-025-61128-y.

[9] K. J. Chaudhary, R. Patel, M. L. Chaudhary, and R. K. Gupta, "Thin-Film Based Photovoltaic Devices," *Handbook of Energy Materials*, pp. 1–28, 2025, doi: 10.1007/978-981-16-4480-1_30-1.

[10] M. A. Green *et al.*, "Solar cell efficiency tables (Version 64)," *Progress in Photovoltaics: Research and Applications*, vol. 32, no. 7, pp. 425–441, Jul. 2024.

[11] "Champion Photovoltaic Module Efficiency Chart | Photovoltaic Research | NREL." Accessed: Nov. 30, 2025. [Online]. Available: https://www.nrel.gov/pv/module-efficiency

[12] A. Machín and F. Márquez, "Advancements in Photovoltaic Cell Materials: Silicon, Organic, and Perovskite Solar Cells," *Materials 2024, Vol. 17, Page 1165*, vol. 17, no. 5, p. 1165, Mar. 2024, doi: 10.3390/MA17051165.

[13] S. Chen, N. Liu, F. Xu, and G. Wei, "Challenges and Strategies Toward Future Stable Perovskite Photovoltaics," *Solar RRL*, vol. 7, no. 23, p. 2300479, Dec. 2023.

[14] "World Energy Outlook 2019 – Analysis - IEA." Accessed: Nov. 29, 2025. [Online]. Available: https://www.iea.org/reports/world-energy-outlook-2019

[15] "Renewable Power Generation Costs in 2020." Accessed: Nov. 29, 2025. [Online]. Available: https://www.irena.org/publications/2021/Jun/Renewable-Power-Costs-in-2020

[16] U. Energy Information Administration, "Levelized Costs of New Generation Resources in the Annual Energy Outlook 2021," 2021.

[17] D. Burkitt *et al.*, "Roll-to-roll slot-die coated P–I–N perovskite solar cells using acetonitrile based single step perovskite solvent system," *Sustain Energy Fuels*, vol. 4, no. 7, pp. 3340–3351, Jun. 2020, doi: 10.1039/D0SE00460J.

[18] A. Verma *et al.*, "Towards industrialization of perovskite solar cells using slot die coating," *J Mater Chem C Mater*,

http://www.doi.org/10.62341/istj-vol38-2-irego74

vol. 8, no. 18, pp. 6124–6135, May 2020, doi: 10.1039/D0TC00327A.

[19] F. De Rossi *et al.*, "All Printable Perovskite Solar Modules with 198 cm2 Active Area and Over 6% Efficiency," *Adv Mater Technol*, vol. 3, no. 11, p. 1800156, Nov. 2018.

[20] L. Gao, K. Huang, C. Long, F. Zeng, B. Liu, and J. Yang, "Fully slot-die-coated perovskite solar cells in ambient condition," *Appl Phys A Mater Sci Process*, vol. 126, no. 6, Jun. 2020, doi: 10.1007/S00339-020-03628-W.

[21] J. E. Kim, S. S. Kim, C. Zuo, M. Gao, D. Vak, and D. Y. Kim, "Humidity-Tolerant Roll-to-Roll Fabrication of Perovskite Solar Cells via Polymer-Additive-Assisted Hot Slot Die Deposition," *Adv Funct Mater*, vol. 29, no. 26, p. 1809194, Jun. 2019.

[22] A. S. Subbiah *et al.*, "High-Performance Perovskite Single-Junction and Textured Perovskite/Silicon Tandem Solar Cells via Slot-Die-Coating," *ACS Energy Lett*, vol. 5, no. 9, pp. 3034–3040, Sep. 2020, doi: 10.1021/ACSENERGYLETT.0C01297.

[23] M. Fievez *et al.*, "Slot-die coated methylammonium-free perovskite solar cells with 18% efficiency," *Solar Energy Materials and Solar Cells*, vol. 230, p. 111189, Sep. 2021.

[24] A. Karavioti, E. Vitoratos, and E. Stathatos, "Improved performance and stability of hole-conductor-free mesoporous perovskite solar cell with new amino-acid iodide cations," *Journal of Materials Science: Materials in Electronics*, vol. 31, no. 8, pp. 6109–6117, Apr. 2020, doi: 10.1007/S10854-020-03164-6.

[25] B. Chen *et al.*, "Blade-Coated Perovskites on Textured Silicon for 26%-Efficient Monolithic Perovskite/Silicon Tandem Solar Cells," *Joule*, vol. 4, no. 4, pp. 850–864, Apr. 2020, doi: 10.1016/J.JOULE.2020.01.008.

[26] J. M. Kadro and A. Hagfeldt, "The End-of-Life of Perovskite PV," *Joule*, vol. 1, no. 1, pp. 29–46, Sep. 2017, doi: 10.1016/J.JOULE.2017.07.013.

[27] G. Schileo and G. Grancini, "Lead or no lead? Availability, toxicity, sustainability and environmental impact of lead-

http://www.doi.org/10.62341/istj-vol38-2-irego74

free perovskite solar cells," *J Mater Chem C Mater*, vol. 9, no. 1, pp. 67–76, Jan. 2021, doi: 10.1039/D0TC04552G.

[28] G. Calvo and A. Valero, "Strategic mineral resources: Availability and future estimations for the renewable energy sector," *Environ Dev*, vol. 41, p. 100640, Mar. 2022, doi: 10.1016/J.ENVDEV.2021.100640.

[29] C. Dong *et al.*, "Carbon-based all-inorganic perovskite solar cells: Progress, challenges and strategies toward 20% efficiency," Nov. 01, 2021, *Elsevier B.V.* doi: 10.1016/j.mattod.2021.05.016.

[30] A. Valero, A. Valero, G. Calvo, and A. Ortego, "Material bottlenecks in the future development of green technologies," *Renewable and Sustainable Energy Reviews*, vol. 93, pp. 178–200, Oct. 2018, doi: 10.1016/J.RSER.2018.05.041.

[31] K. P. Goetz, A. D. Taylor, Y. J. Hofstetter, and Y. Vaynzof, "Sustainability in Perovskite Solar Cells," *ACS Appl Mater Interfaces*, vol. 13, no. 1, pp. 1–17, Jan. 2020, doi: 10.1021/ACSAMI.0C17269.